Research Article

3-Mercaptopropionic, 4-Mercaptobenzoic, and Oleic Acid-Capped CdSe Quantum Dots: Interparticle Distance, Anchoring Groups, and Surface Passivation

José Augusto Lucena dos Santos,[1] **Fabio Baum,**[2] **Emerson Cristofer Kohlrausch,**[2] **Fabiele C. Tavares,**[2] **Tatiane Pretto,**[1] **Francisco P. dos Santos,**[1] **Jacqueline F. Leite Santos,**[1,2] **Sherdil Khan** (ID) **,**[2,3] **and Marcos J. Leite Santos** (ID) [1,2]

[1]*Instituto de Química, Universidade Federal do Rio Grande do Sul, 91501-970 Porto Alegre, RS, Brazil*
[2]*Programa de Pos-Graduação em Ciências de Materiais, Universidade Federal do Rio Grande do Sul, 91501-970 Porto Alegre, RS, Brazil*
[3]*Instituto de Física, Universidade Federal do Rio Grande do Sul, Av. Bento Goncalves, 9500 Porto Alegre, RS, Brazil*

Correspondence should be addressed to Sherdil Khan; sherdil.khan@ufrgs.br

The optoelectronic properties of quantum dots are strongly controlled by the chemical nature of their surface-passivating ligands. In this work, we present the synthesis, characterization, and surface modification of CdSe quantum dots (QDs) and their application in solar cells. CdSe QDs were capped in oleic acid (OA), 3-mercaptopropionic acid (MPA), and 4-mercaptobenzoic acid (MBA). The QDs were characterized by transmission electron microscopy (TEM), UV-Vis absorption and emission spectrophotometry, thermogravimetric analyses, and ^{1}H and ^{13}C NMR. From TEM analysis, it has been observed that interparticle distance can be effectively controlled by the presence of different molecular size ligands. From the ^{1}H and ^{13}C NMR, specific types of interactions between the Cd^{2+} and the ligands have been observed. Although CdSe/OA presented larger interparticle distance as compared to CdSe/MPA and CdSe/MBA, the photocatalytic oxidation of the thiol groups on the surface of the MPA- and MBA-based quantum dots resulted in poor surface stabilization, ultimately resulting in poor power conversion efficiencies which were ca. 70% smaller than that of OA-based solar cell.

1. Introduction

Within the last 30 years the research on quantum dots (QDs) has shown a strong impact in chemistry, physics, and medical science; these nanomaterials have been largely applied in the development of assays, bioprobes, sensors, LEDs, solar cells, and TVs [1–10]. In the nanoscale realm, the behavior of the devices and related phenomena are surface dependent. Since QDs present high surface-to-volume ratio; therefore, surface functionalization is one of the most crucial parameters to be addressed [11–20]. The literature shows studies on a large group of molecules that strongly bind to inorganic surfaces through a Lewis base anchoring group such as thiol [21], carboxylate [12], phosphonate [10, 22], and amine, which bind to the empty orbitals of inorganic elements [22]. These molecules stabilize the particles during the synthesis, control their shape and size distribution which influence their interaction with each other and with the surroundings, and ultimately control their solubility and potential to binding events [23–26]. In addition, the stabilizing agents passivate surface electronic states and defects in semiconductors, contributing to the reduction of trapping states [27–29].

Concerning application in solar cells, the effect of surface ligands has been widely studied for several QDs and ligands. Previous results show that passivation is strongly dependent

on the ligand, resulting in either improvement or drop of power conversion efficiency [30–33]. Usually, large molecular size ligands such as oleic acid are required to maintain colloidal stability in organic solvents; however, for application in systems that require electronic transport among the QDs, such as in solar cells, a ligand exchange from long to short ligands is desirable in order to decrease the spacing among the QDs improving electronic transport [33–37]. Hence, in order to obtain quantum dots with improved optoelectronic properties, one should obtain stable particles presenting good electronic transport.

Among many cadmium chalcogenide semiconductors, CdSe quantum dots have been widely studied in the literature [38–42]. Cadmium chalcogenides are well-known for their synthesis, yields, reliability, and stability. Their synthesis usually requires high temperature of ca. 240°C which necessitates the addition of stable organic ligands having high boiling point in addition to their solubility in the reaction medium. In addition, the ligands should have at least one group with high electronic density, which can bind to the particle surface. The Cd^{2+} binding helps to control the shape and prevents the agglomeration and uncontrolled growth of the quantum dots.

Two-phase ligand exchange is a well-known procedure to functionalize quantum dot surface [43, 44]. This process is analogous to nucleophilic substitution reactions in coordinating complexes. This approach classifies the ligands in three different types: L, X, and Z type. The L type ligands are charge neutral two electron donors with a lone pair, such as amines, phosphines, and carboxylic acids which bond to the electron-deficient surface sites of the nanocrystal. The X type has an odd negative charge, such as oleates, thiolates, and phosphonates, and requires one electron from the surface of the nanocrystal to form a two-electron covalent bond. Finally, the Z type interacts with the surface of the nanocrystal as electron acceptors [45]. In the case of CdSe QDs, the ligands, such as oleic acid (L) and oleate (X), are bound to the metallic Cd^{2+} sites onto the QD surface [45]. In the case of L type ligand exchange, in the room temperature, the charge neutral ligands are constantly adsorbing and desorbing on the surface of the nanocrystal, and they are low cost. However, for the X type ligands, there is a formation of an electrostatic charged site when the ligand leaves the surface of the nanocrystal. Earlier works presented that basic environment is more favorable to promote the ligand exchange from oleates to thiol linking groups [46] probably due to the charge stabilization of the surface during the leaving of the X type ligand [43, 45, 47]. Understanding the functionalization of QDs with these three ligands is very important and warrants a systematic study. Although several spectroscopic techniques have been used to the characterization of surface ligands on QD surface at the molecular scale, nevertheless, nuclear magnetic resonance (NMR) is the most robust method to study ligand binding [48–50]. Hence, in this work NMR allowed us to evaluate how the different ligands are bound to the QD surface, and how they affect the QD optical properties.

This paper describes a study on three different ligands, aimed at improving the minimum interparticle distance required to yield optically interesting materials that maintain the quantum confinement properties.

2. Materials and Methods

2.1. Synthesis of CdSe. Oleic acid-capped CdSe quantum dots (CdSe/OA) were synthesized by using hot injection. In a three-neck flask, 0.5 mmol of cadmium acetate dihydrate, 5 mmol of oleic acid, and 10 mL of octadecene were added and degassed under vacuum at 80°C, until the formation of bubbles was no longer observed. The solution was heated to the reaction temperature of 240°C. In another flask, 0.05 g of selenium powder and 2 mL of trioctylphosphine were mixed, heated to 60°C, and kept under stirring until it became optically clear. This solution was injected into the three-neck flask; the reaction was allowed for 2 minutes and stopped by immersion in a cold bath. The resultant solution was precipitated with acetone and centrifuged at 2.000 rpm. The precipitated was dispersed in hexane and the process was repeated.

2.2. Ligand Exchange. (CdSe/OA) in either mercaptopropionic acid (MPA) or mercaptobenzoic acid (MBA) were mixed with 5 mL of methanol, keeping a mass ratio of 1 : 2 (CdSe/OA)/MPA or MBA. The pH was adjusted to 11.0 by using tetramethylammonium hydroxide. After ligand exchange, the CdSe was precipitated with ethyl acetate and separated by centrifugation.

2.3. Solubility. Solubility tests were carried out after ligand exchange, by adding polar solvents, such as water, ethanol, or methanol, to confirm the replacement of oleic acid by MPA or MBA.

2.4. Quantum Dot Characterization. UV-Vis spectroscopy was carried out on a Shimadzu UV-2450 spectrometer within the wavelength range between 300 and 700 nm, using a standard 10 mm quartz cuvette. The emission spectra were measured in the same range in a Varian spectrofluorometer. TEM images were obtained in a JEOL JEM 1200 EXII operating at 80 kV. A Bruker Avance 400 MHz, equipped with BBO probe of 5 mm with direct detection, was used to obtain the NMR (^{1}H and ^{13}C) spectra. Frequencies of 400 MHz and 100 MHz were used for ^{1}H and ^{13}C, respectively. The solvents were D_2O and $CDCl_3$ for MBA- and MPA-capped nanoparticles and OA-capped nanoparticles, respectively. The thermal properties were characterized by thermogravimetric analysis performed in a TGA Q5000IR, programmed in a heating rate of 10°C/min from 0 to 800°C with a nitrogen flow of 100 mL/min.

2.5. Quantum Dot Sensitized Solar Cell Assembly. The TiO_2 paste [51] was screen-printed on a transparent conductive substrate (FTO), previously immersed in 40 mmol·L^{-1} $TiCl_4$ aqueous solution at 80°C for 30 minutes. The substrate was heated on a hot plate at 125°C for 6 minutes, following the heat treatment to 500°C for sintering. After cooling down to 60°C, the substrates were immersed in the sensitizer solution for 24 hours. The counter electrodes were prepared by coating the FTO surface by CuS obtained by electrochemical

route [44]. The electrolyte was prepared by dissolving 1.0 M of Na_2S and 0.125 M of S in deionized water. The solar cell was sealed by using Meltonix, a polymeric film of low melting temperature. The devices were labeled as TiO_2/CdSe/OA, TiO_2/CdSe/MBA, and TiO_2/CdSe/MPA.

2.6. Device Characterization. Current vs. potential curves were acquired in the potential ranging from −0.4 to +0.8 V, using a Xenon lamp of 300 W adjusted to 100 mW·cm^{-2} in an electrometer (Source Meter Keithley 2410).

3. Results and Discussion

Figure 1 presents the comparison between absorption and emission spectra of the as-synthesized OA-capped QDs and after ligand exchange for either MPA or MBA. As one can observe, the absorption peak of MPA- and MBA-capped QDs is redshifted when compared to the as-synthesized OA-capped QDs. This result suggests a formation of a ligand monolayer on the surface of the QD, causing a relaxation on the quantum confinement effect [52]. In addition, there is a reduction of the Stokes shift from the OA-capped QDs to the thiol-capped QDs as presented in Figure 1.

Previous works reported a relation between the reduction of the Stokes shift and increase in the fluorescence quantum yield, elaborating that samples with smaller Stokes shifts present a better surface trapping state passivation [52, 53]. The improved surface passivation of CdSe can be explained in terms of the HSAB theory [54, 55]. As Cd^{2+} from the CdSe is a soft acid and the oleate ligand is a hard base, there is a weak bond on the QD surface. After ligand exchange, the soft Cd^{2+} is combined with the hard base thiol (SH), leading to a stronger interaction and better passivation.

TEM images of the CdSe quantum dots show the formation of nearly spherical particles (Figure 2), presenting a nearly narrow size distribution, with an average size of 4.5 nm. An interesting result from the quantum dots encapsulated by oleic acid is the homogeneous interparticle spacing, with an average of 1.9 nm, controlled by the passivation layer. As one can observe, there is an agglomeration of the quantum dots when OA is exchanged by MPA and MBA. This behavior can be explained by the photocatalytic oxidation of the thiol groups on the surface of the quantum dots. Once oxidized, the thiol forms disulfides, which do not bind efficiently to the surface of the nanocrystal; therefore, it drops into the solution [46]. As the reaction progresses, the particles start to agglomerate, without significantly changing the nanocrystal size and distribution as observed in the UV-Vis absorption spectra (Figure 1). It was earlier demonstrated that the agglomeration rate is a strong function of the carbon chain length of the ligand, either because of the energetic barrier due to the interaction among the ligand monolayer or the repulsive potential between the two spheres, enhanced by the monolayer thickness of the ligands, as demonstrated by Biermann et al. [41]. The molecular chain length ($D_{molecule}$) of OA (1.937 nm), MPA (0.409 nm), and MBA (0.596 nm) contributes to explain the behavior shown in Figures 2(b), 2(d), and 2(f) where $D_{molecule}$ of each ligand is compared to the dispersion of the quantum dots.
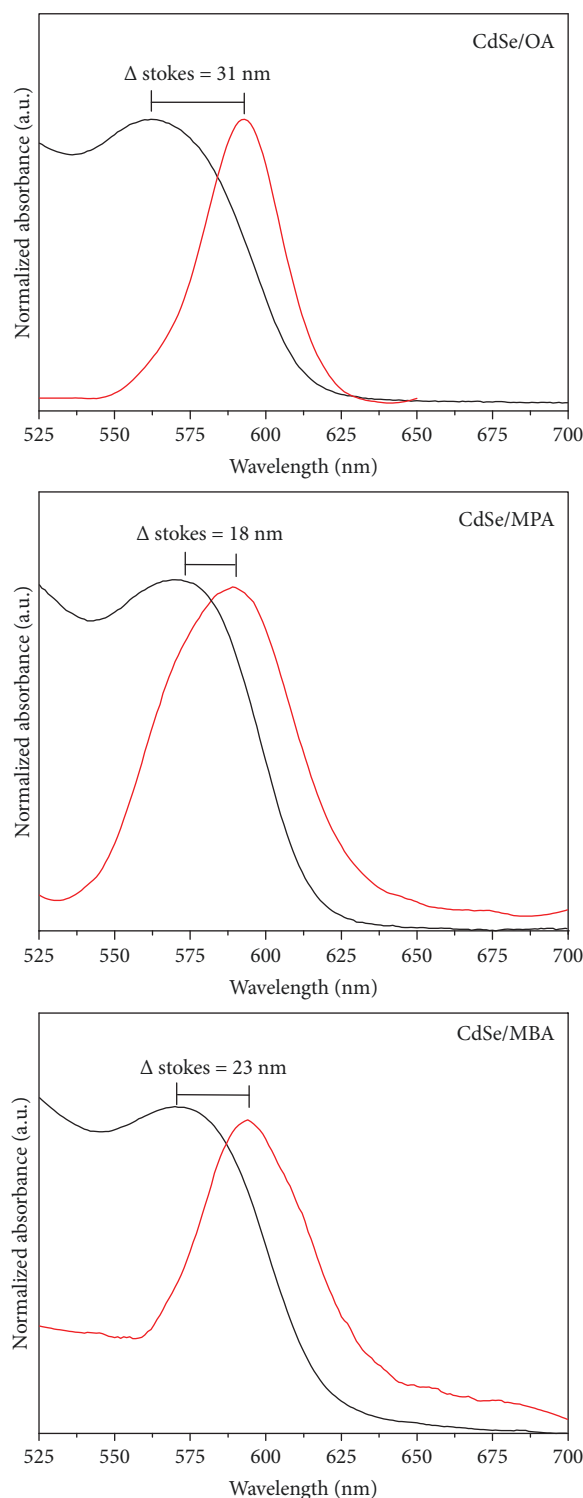

FIGURE 1: Absorption (black line) and emission (red line) spectra of CdSe/OA, CdSe/MPA, and CdSe/MBA.

Ligand exchange on the surface of the quantum dots was further investigated by thermogravimetric (TGA) and derivative thermogravimetric (DTG) analyses (Figure 3). Figure 3(a) presents the TGA and DTG from CdSe/OA. The first DTG peak, at ca. 435°C, with a 34.5% loss from the initial mass, is characteristic of molecules which interacts
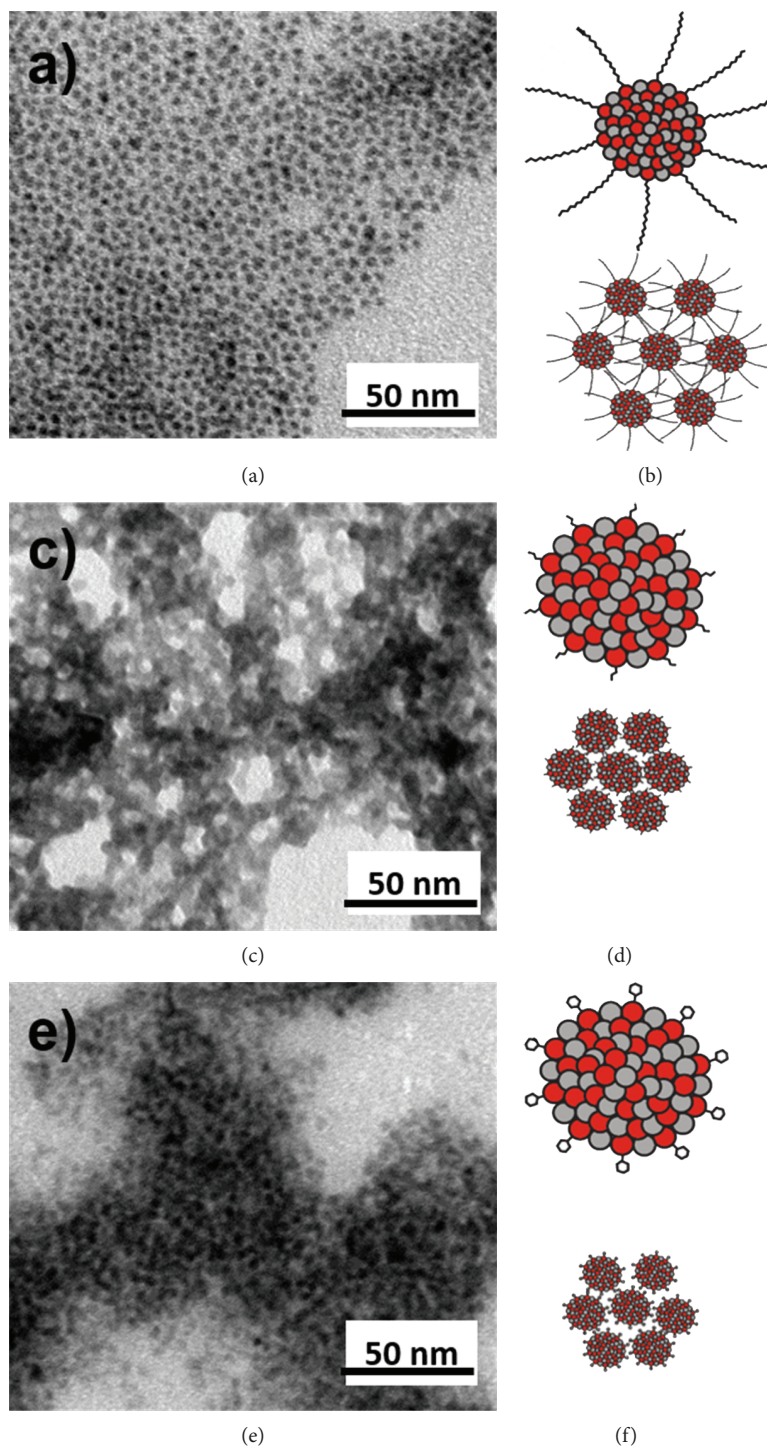
(a)

(b)

(c)

(d)

(e)

(f)

FIGURE 2: TEM images of CdSe quantum dots with OA, MPA, and MBA (a, c, e). Comparison of interparticle space between OA-capped CdSe QDs (b), MPA-capped CdSe QDs (d), and MBA-capped CdSe QDs (f).

with the quantum dots through the carbonyl, such as OA [56–58]. A minor peak was also observed at 575°C, with mass loss of 4.2%. The thermogram from CdSe/MPA (Figure 3(b)) shows a loss of 12.0% within a large range from 165 to 400°C. The DTG peak at 235°C, the small shoulder at 295°C, a 3.3% mass loss between 540 and 800°C and a small peak at 600°C, gives the total mass loss of 15.3%.

For the CdSe/MBA (Figure 3(c)), it is possible to observe two main peaks in the DTG, one at 272°C, with a mass loss of 10.5%, and the other at 415°C, with a mass loss of 4.6%. In addition, a small peak is seen at 620°C, with a mass loss of 3.2%, resulting in a total mass loss of 18.3%. Additionally, CdSe/MPA and CdSe/MBA (Figures 3(b) and 3(c)) show some initial mass loss at around 50°C, probably related to
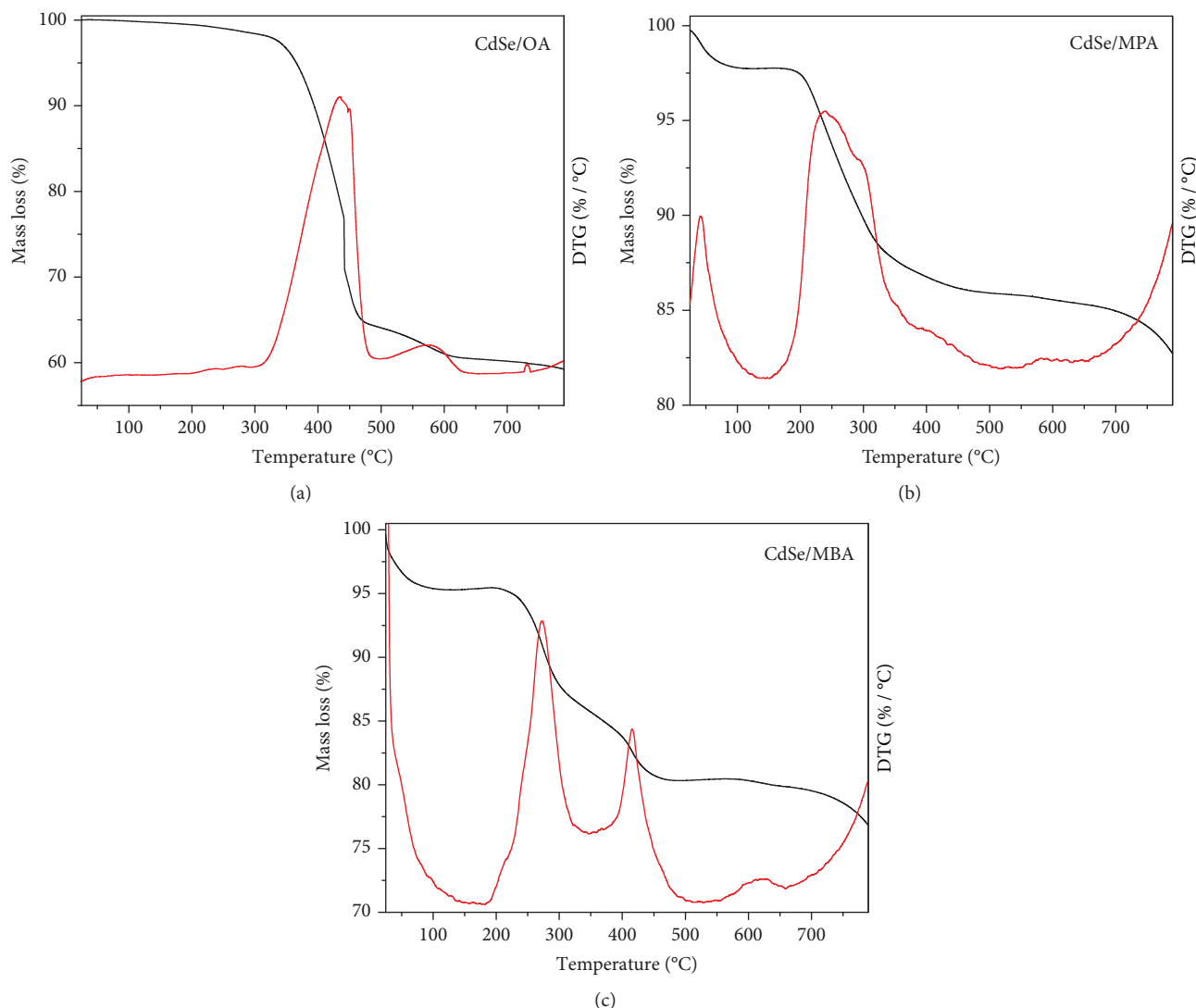
FIGURE 3: TGA/DTG of CdSe quantum dots capped with (a) OA, (b) MPA, and (c) MBA.

the methanol solvent, employed in the ligand exchange process. The small losses above 500°C may be related to the loss of CdSe itself, as already reported on thermal treatment experiments with ligand-free CdSe nanocrystals [4]. The analysis of the percentages of total lost mass (Table 1) shows that there is a correlation between the total mass loss and the molar weight of ligands of the quantum dots. Compared to others, the CdSe/OA presented the highest total mass loss; these results indicate that higher amount of OA took part in the surface passivation due to the presence of carbonyl group which might be one more reason of increased interparticle distance observed in the TEM image of this sample (Figure 2(a)). In addition, the CdSe/OA sample presented the largest Stokes shift (Figure 1) which might be related to the presence of these carbonyl groups, higher content of which might act as light scattering centers.

3.1. NMR Analysis of the Ligands. The comparison between the ^{1}H and ^{13}C NMR spectra of pure MPA and CdSe/MPA shows at least two types of different intermolecular

TABLE 1: Relation between sample and total mass loss for each ligand.

Sample	Peak DTG 1 (°C)	Loss mass 1 (%)	Peak DTG 2 (°C)	Loss mass 2 (%)	Peak DTG 3 (°C)	Loss mass 3 (%)	Total mass loss
CdSe/OA	435	34.5	575	4.2			38.7%
CdSe/MPA	235	10.2	295	1.8	600	3.3	15.3%
CdSe/MBA	272	10.5	415	4.6	620	3.2	18.3%

interactions. In the ^{1}H-NMR spectrum of pure MPA, the two signals of hydrogen in the CH_2 groups (H_2 and H_3) are overlapped, and the hydrogen of the SH group presents itself as a triplet, due to the coupling constant $^3J_{H_4H_3}$, with a chemical shift of 1.64 ppm. However, the spectrum of CdSe/MPA ^{1}H-NMR (Figure S1—Supplementary Materials) shows a significant change on the chemical shift of CH_2 and SH group. There is a separation of the different signals referring to the two CH_2 groups (H_2 and H_3) and they

present triplet signals due to the coupling constant $^3J_{H_2H_3}$ between them. The signal referring to the H_4 (SH group) changed to a singlet with a chemical shift of 1.92 ppm. The increasing of the frequency of the signal and the elimination of the coupling between H_4 and H_3 ($^3J_{H_4H_3} = 0$) are due to the interaction between sulfur and cadmium. In this case, the metal behaves as a Lewis acid and interacts with the ligand through the sulfur atom. This causes the loss of electronic shielding of H_4, the increase of its frequency on the ^{1}H-NMR spectrum influences the mechanism of the coupling constant $^3J_{H_4H_3}$, which is not observed anymore. The ^{13}C-NMR spectrum of the CdSe/MPA presents an interesting result (Figure S2—Supplementary Materials). We observe two different signals to the carbonyl carbon. Both carbonyl carbon signals have higher chemical displacement than the carbonyl signal of the pure ligand. The presence of two carbonyl carbon signals with higher frequency on the ^{13}C-NMR spectra of CdSe/MPA suggests that the cadmium actuates as a Lewis acid in the interaction with the ligand. In addition, there is an interaction between Cd-S, observed on the ^{1}H-NMR spectrum, and between the ligand carbonyl group and the cadmium. The two carbonylic signals are due to an interaction between Cd-S and Cd-COOH. The ^{1}H-NMR spectrum of the CdSe/MBA (Figure S3—Supplementary Materials) showed the presence of at least three different sets of ligand molecules, suggesting three different types of interactions between the CdSe and the ligand. The overlap between the ^{1}H-NMR for the pure ligand and the CdSe/MBA (Figure S4—Supplementary Materials) presents the expansion of the aromatic hydrogen region for the pristine ligand and the CdSe/MBA. The three different sets of signals of aromatic hydrogen for the ligand on the quantum dot strongly suggest three types of interaction between the cadmium and the ligand molecules. Probably, there is an interaction between the Lewis acid and the carbonyl group, the Lewis acid and the SH group, and a third interaction π-stack type between Lewis acid and aromatic π system. Based on the above analyses, we have depicted different types of interaction between the nanoparticle and the ligands (Figure 4). The ^{13}C-NMR spectrum shows a large amount of aromatic signals related to the different ligand molecules interacting with the CdSe. In addition, in this case, three carbonyl carbon signals were noticed, corroborating the three types of observed ligand molecules. The behavior of the spectra of ^{1}H-NMR and ^{13}C-NMR for MPA and MBA as CdSe ligands leads to the conclusion that these ligands have different ways of fixing to the surface of the quantum dot.

Figure 5 shows the current versus potential curves from the solar cells assembled with CdSe/OA, CdSe/MPA, and CdSe/MBA. The ligand does not promote a significant change on the quasi-fermi level of the system TiO$_2$/quantum dot; hence, the open-circuit potential is found independent of the ligand. It should be noted that thinner ligand shells should directly improve carrier transport properties. MBA and MPA present the shortest chain lengths and smaller interparticle distances (Figure 1), from which one can expect faster electron transfer rate to TiO$_2$ and hence better device
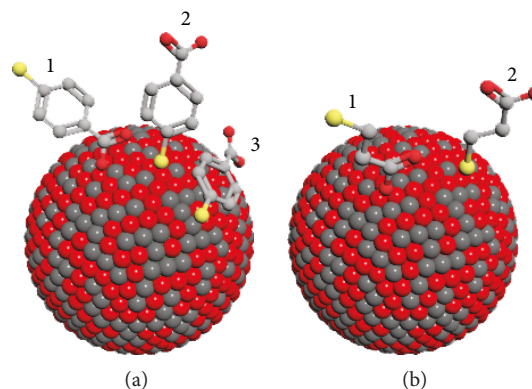

(a)   (b)

Figure 4: (a) Representation of the CdSe-MBA interaction, with the π stacking-metal interaction (1), the thiol-metal interaction (2), and the carbonyl-metal interaction (3). (b) CdSe-MPA interaction, with the thiol-metal (1) and the carbonyl-metal (2) interaction.
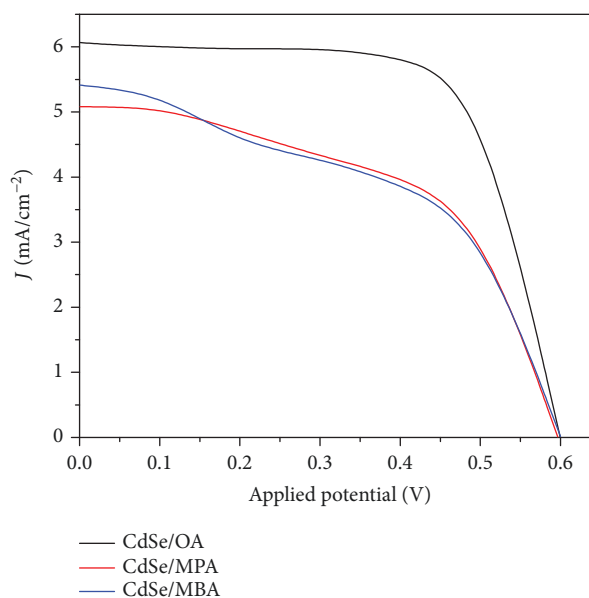

Figure 5: Current vs. potential curves of solar cells sensitized with CdSe/OA, CdSe/MPA, and CdSe/MBA.

performance [59–61]. However, the highest photocurrent is obtained from the quantum dots capped with oleic acid. The decrease in the performance of the devices assembled with CdSe/MPA and CdSe/MBA is related to the agglomeration of the quantum dots when OA is exchanged by MPA and MBA.

Table 2 shows the short-circuit current (I_{sc}), open-circuit voltage (V_{oc}), Fill Factor (FF), and efficiency (η) obtained from the assembled devices. The power conversion efficiencies (at AM 1.5G illumination) of CdSe/OA, CdSe/MPA, and CdSe/MBA were 2.70%, 1.69%, and 1.60%, respectively.

4. Conclusions

The optical measurements of the QDs in solution suggest better surface passivation for surface trapping states with MBA and MPA rather than using OA. However, photocatalytic

TABLE 2: Electrical parameters of the assembled devices.

Devices	I_{sc} (mA)	V_{oc} (V)	$I_{max} \cdot V_{max}$	FF	η
CdSe/OA	6.05	0.6	2.70	73%	2.70%
CdSe/MPA	5.08	0.6	1.69	55%	1.69%
CdSe/MBA	5.41	0.6	1.60	49%	1.60%

oxidation of the thiol groups on the surface of the QDs results in lower colloidal stability, hence resulting in QD aggregation on the TiO$_2$ mesoporous film. The OA molecule well stabilizes the CdSe against agglomeration, increasing QD loading and light harvesting, in addition to suppress the recombination of separated charges. The overall power conversion efficiency of devices assembled with OA-capped CdSe showed ca. 70% improvement over the devices assembled with CdSe capped with MPA and MBA.

Data Availability

All the data used in this study are provided in Results and Discussion and the supporting information of this paper as well.

Conflicts of Interest

The authors declare that there is no conflict of interest regarding the publication of this paper.

Acknowledgments
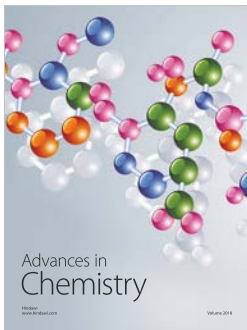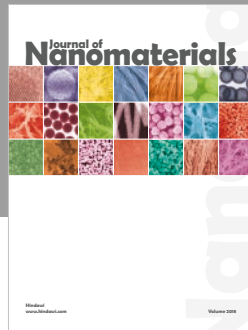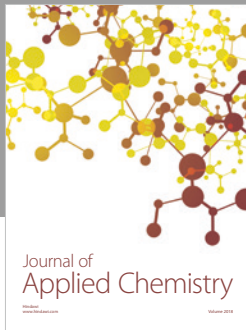
Supplementary Materials

Figures S1-S4: ^{1}H and ^{13}C NMR analyses. (Supplementary Materials)

References

[1] M. Bruchez Jr., M. Moronne, P. Gin, S. Weiss, and A. P. Alivisatos, "Semiconductor nanocrystals as fluorescent biological labels," *Science*, vol. 281, no. 5385, pp. 2013–2016, 1998.

[2] D. Cadeddu, M. Munsch, N. Rossi et al., "Electric-field sensing with a scanning fiber-coupled quantum dot," *Physical Review Applied*, vol. 8, no. 3, 2017.

[3] M. J. L. Santos, J. Ferreira, E. Radovanovic, R. Romano, O. L. Alves, and E. M. Girotto, "Enhancement of the photoelectrochemical response of poly(terthiophenes) by CdS(ZnS) core-shell nanoparticles," *Thin Solid Films*, vol. 517, no. 18, pp. 5523–5529, 2009.

[4] J. A. Fernandes, P. Migowski, Z. Fabrim et al., "TiO$_2$ nanotubes sensitized with CdSe via RF magnetron sputtering for photoelectrochemical applications under visible light irradiation," *Physical Chemistry Chemical Physics*, vol. 16, no. 19, pp. 9148–9153, 2014.

[5] I. L. Medintz, H. T. Uyeda, E. R. Goldman, and H. Mattoussi, "Quantum dot bioconjugates for imaging, labelling and sensing," *Nature Materials*, vol. 4, no. 6, pp. 435–446, 2005.

[6] Z. Yue, F. Lisdat, W. J. Parak et al., "Quantum-dot-based photoelectrochemical sensors for chemical and biological detection," *ACS Applied Materials & Interfaces*, vol. 5, no. 8, pp. 2800––2814, 2013.

[7] R. Gill, M. Zayats, and I. Willner, "Semiconductor quantum dots for bioanalysis," *Angewandte Chemie International Edition*, vol. 47, no. 40, pp. 7602–7625, 2008.

[8] I. L. Medintz and H. Mattoussi, "Quantum dot-based resonance energy transfer and its growing application in biology," *Physical Chemistry Chemical Physics*, vol. 11, no. 1, pp. 17–45, 2009.

[9] D. Cadeddu, J. Teissier, F. R. Braakman et al., "A fiber-coupled quantum-dot on a photonic tip," *Applied Physics Letters*, vol. 108, no. 1, article 011112, 2016.

[10] L. J. Brennan, F. Purcell-Milton, B. McKenna, T. M. Watson, Y. K. Gun'ko, and R. C. Evans, "Large area quantum dot luminescent solar concentrators for use with dye-sensitised solar cells," *Journal of Materials Chemistry A*, vol. 6, no. 6, pp. 2671–2680, 2018.

[11] R. Bilan, F. Fleury, I. Nabiev, and A. Sukhanova, "Quantum dot surface chemistry and functionalization for cell targeting and imaging," *Bioconjugate Chemistry*, vol. 26, no. 4, pp. 609––624, 2015.

[12] R. A. Sperling and W. J. Parak, "Surface modification, functionalization and bioconjugation of colloidal inorganic nanoparticles," *Philosophical Transactions of the Royal Society A: Mathematical, Physical and Engineering Sciences*, vol. 368, no. 1915, pp. 1333–1383, 2010.

[13] L. O. Cinteza, "Quantum dots in biomedical applications: advances and challenges," *Journal of Nanophotonics*, vol. 4, no. 1, 2010.

[14] L. Manna, E. C. Scher, L. S. Li, and A. P. Alivisatos, "Epitaxial growth and photochemical annealing of graded CdS/ZnS shells on colloidal CdSe nanorods," *Journal of the American Chemical Society*, vol. 124, no. 24, pp. 7136–7145, 2002.

[15] M. S. Muthu, S. A. Kulkarni, A. Raju, and S. S. Feng, "Theranostic liposomes of TPGS coating for targeted co-delivery of docetaxel and quantum dots," *Biomaterials*, vol. 33, no. 12, pp. 3494–3501, 2012.

[16] A. M. Derfus, W. C. W. Chan, and S. N. Bhatia, "Intracellular delivery of quantum dots for live cell labeling and organelle tracking," *Advanced Materials*, vol. 16, no. 12, pp. 961–966, 2004.

[17] A. S. Karakoti, R. Shukla, R. Shanker, and S. Singh, "Surface functionalization of quantum dots for biological applications," *Advances in Colloid and Interface Science*, vol. 215, pp. 28–45, 2015.

[18] H. Sohn, S. Létant, M. J. Sailor, and W. C. Trogler, "Detection of fluorophosphonate chemical warfare agents by catalytic hydrolysis with a porous silicon interferometer," *Journal of the American Chemical Society*, vol. 122, no. 22, pp. 5399-5400, 2000.

[19] X. Wang, Zhang, Niehaus, and T. Frauenheim, "Excited state properties of allylamine-capped silicon quantum dots," *The*

Journal of Physical Chemistry C, vol. 111, no. 6, pp. 2394–2400, 2007.

[20] C. B. Murray, C. R. Kagan, and M. G. Bawendi, "Synthesis and characterization of monodisperse nanocrystals and close-packed nanocrystal assemblies," *Annual Review of Materials Science*, vol. 30, no. 1, pp. 545–610, 2000.

[21] H. Döllefeld, K. Hoppe, J. Kolny, K. Schilling, H. Weller, and A. Eychmüller, "Investigations on the stability of thiol stabilized semiconductor nanoparticles," *Physical Chemistry Chemical Physics*, vol. 4, no. 19, pp. 4747–4753, 2002.

[22] D. V. Leff, L. Brandt, and J. R. Heath, "Synthesis and characterization of hydrophobic, organically-soluble gold nanocrystals functionalized with primary amines," *Langmuir*, vol. 12, no. 20, pp. 4723–4730, 1996.

[23] T. Sakura, T. Takahashi, K. Kataoka, and Y. Nagasaki, "One-pot preparation of mono-dispersed and physiologically stabilized gold colloid," *Colloid & Polymer Science*, vol. 284, no. 1, pp. 97–101, 2005.

[24] M. Green, "The nature of quantum dot capping ligands," *Journal of Materials Chemistry*, vol. 20, no. 28, p. 5797, 2010.

[25] Z. A. Peng and X. Peng, "Mechanisms of the shape evolution of CdSe nanocrystals," *Journal of the American Chemical Society*, vol. 123, no. 7, pp. 1389–1395, 2001.

[26] C. Burda, X. Chen, R. Narayanan, and M. A. El-Sayed, "Chemistry and properties of nanocrystals of different shapes," *Chemical Reviews*, vol. 105, no. 4, pp. 1025–1102, 2005.

[27] Z. Jin, A. Wang, Q. Zhou, Y. Wang, and J. Wang, "Detecting trap states in planar PbS colloidal quantum dot solar cells," *Scientific Reports*, vol. 6, no. 1, article 37106, 2016.

[28] C.-H. M. Chuang, P. R. Brown, V. Bulović, and M. G. Bawendi, "Improved performance and stability in quantum dot solar cells through band alignment engineering," *Nature Materials*, vol. 13, no. 8, pp. 796–801, 2014.

[29] G.-H. Kim, F. P. García de Arquer, Y. J. Yoon et al., "High-efficiency colloidal quantum dot photovoltaics via robust self-assembled monolayers," *Nano Letters*, vol. 15, no. 11, pp. 7691–7696, 2015.

[30] R. Wang, Y. Shang, P. Kanjanaboos, W. Zhou, Z. Ning, and E. H. Sargent, "Colloidal quantum dot ligand engineering for high performance solar cells," *Energy & Environmental Science*, vol. 9, no. 4, pp. 1130–1143, 2016.

[31] R. Azmi, S. Sinaga, H. Aqoma et al., "Highly efficient air-stable colloidal quantum dot solar cells by improved surface trap passivation," *Nano Energy*, vol. 39, pp. 86–94, 2017.

[32] M. S. de la Fuente, R. S. Sánchez, V. González-Pedro et al., "Effect of organic and inorganic passivation in quantum-dot-sensitized solar cells," *The Journal of Physical Chemistry Letters*, vol. 4, no. 9, pp. 1519–1525, 2013.

[33] G. H. Carey, A. L. Abdelhady, Z. Ning, S. M. Thon, O. M. Bakr, and E. H. Sargent, "Colloidal quantum dot solar cells," *Chemical Reviews*, vol. 115, no. 23, pp. 12732–12763, 2015.

[34] Y. Ye, X. Wang, S. Ye, Y. Xu, Z. Feng, and C. Li, "Charge-transfer dynamics promoted by hole trap states in CdSe quantum dots–Ni^{2+} photocatalytic system," *The Journal of Physical Chemistry C*, vol. 121, no. 32, pp. 17112–17120, 2017.

[35] M.-Y. Huang, X.-B. Li, Y.-J. Gao et al., "Surface stoichiometry manipulation enhances solar hydrogen evolution of CdSe quantum dots," *Journal of Materials Chemistry A*, vol. 6, no. 14, pp. 6015–6021, 2018.

[36] A. Y. Nazzal, L. Qu, X. Peng, and M. Xiao, "Photoactivated CdSe nanocrystals as nanosensors for gases," *Nano Letters*, vol. 3, no. 6, pp. 819–822, 2003.

[37] A. E. Colbert, W. Wu, E. M. Janke, F. Ma, and D. S. Ginger, "Effects of ligands on charge generation and recombination in hybrid polymer/quantum dot solar cells," *The Journal of Physical Chemistry C*, vol. 119, no. 44, pp. 24733–24739, 2015.

[38] S. G. McAdams, D. J. Lewis, P. D. McNaughter et al., "High magnetic relaxivity in a fluorescent CdSe/CdS/ZnS quantum dot functionalized with MRI contrast molecules," *Chemical Communications*, vol. 53, no. 76, article 10500, 10503 pages, 2017.

[39] W. R. Algar, A. J. Tavares, and U. J. Krull, "Beyond labels: a review of the application of quantum dots as integrated components of assays, bioprobes, and biosensors utilizing optical transduction," *Analytica Chimica Acta*, vol. 673, no. 1, pp. 1–25, 2010.

[40] P. Maity, T. Debnath, and H. N. Ghosh, "Ultrafast charge carrier delocalization in CdSe/CdS quasi-type II and CdS/CdSe inverted type I core–shell: a structural analysis through carrier-quenching study," *The Journal of Physical Chemistry C*, vol. 119, no. 46, pp. 26202––26211, 2015.

[41] A. Biermann, T. Aubert, P. Baumeister, E. Drijvers, Z. Hens, and J. Maultzsch, "Interface formation during silica encapsulation of colloidal CdSe/CdS quantum dots observed by in situ Raman spectroscopy," *The Journal of Chemical Physics*, vol. 146, no. 13, article 134708, 2017.

[42] O. Friedman, D. Korn, V. Ezersky, and Y. Golan, "Chemical epitaxy of CdSe on GaAs," *CrystEngComm*, vol. 19, no. 36, pp. 5381–5389, 2017.

[43] W. C. Chan and S. Nie, "Quantum dot bioconjugates for ultrasensitive nonisotopic detection," *Science*, vol. 281, no. 5385, pp. 2016–2018, 1998.

[44] F. Wang, H. Dong, J. Pan, J. Li, Q. Li, and D. Xu, "One-step electrochemical deposition of hierarchical CuS nanostructures on conductive substrates as robust, high-performance counter electrodes for quantum-dot-sensitized solar cells," *The Journal of Physical Chemistry C*, vol. 118, no. 34, pp. 19589–19598, 2014.

[45] M. A. Boles, D. Ling, T. Hyeon, and D. V. Talapin, "The surface science of nanocrystals," *Nature Materials*, vol. 15, pp. 141–153, 2016.

[46] Y. Shen, M. Abolhasani, Y. Chen et al., "In-situ microfluidic study of biphasic nanocrystal ligand-exchange reactions using an oscillatory flow reactor," *Angewandte Chemie International Edition*, vol. 56, no. 51, pp. 16333–16337, 2017.

[47] N. Erathodiyil and J. Y. Ying, "Functionalization of inorganic nanoparticles for bioimaging applications," *Accounts of Chemical Research*, vol. 44, no. 10, pp. 925–935, 2011.

[48] E. A. Baquero, W.-S. Ojo, Y. Coppel et al., "Identifying short surface ligands on metal phosphide quantum dots," *Physical Chemistry Chemical Physics*, vol. 18, no. 26, pp. 17330–17334, 2016.

[49] B. Zeng, G. Palui, C. Zhang et al., "Characterization of the ligand capping of hydrophobic CdSe–ZnS quantum dots using NMR spectroscopy," *Chemistry of Materials*, vol. 30, no. 1, pp. 225–238, 2018.

[50] E. Barile and M. Pellecchia, "NMR-based approaches for the identification and optimization of inhibitors of protein–

protein interactions," *Chemical Reviews*, vol. 114, no. 9, pp. 4749–4763, 2014.

[51] S. Ito, T. N. Murakami, P. Comte et al., "Fabrication of thin film dye sensitized solar cells with solar to electric power conversion efficiency over 10%," *Thin Solid Films*, vol. 516, no. 14, pp. 4613–4619, 2008.

[52] F. O. Silva, M. S. Carvalho, R. Mendonça et al., "Effect of surface ligands on the optical properties of aqueous soluble CdTe quantum dots," *Nanoscale Research Letters*, vol. 7, no. 1, p. 536, 2012.

[53] A. L. Rogach, T. Franzl, T. A. Klar et al., "Aqueous synthesis of thiol-capped CdTe nanocrystals: state-of-the-art," *The Journal of Physical Chemistry C*, vol. 111, no. 40, pp. 14628–14637, 2007.

[54] R. G. Pearson, "Hard and soft acids and bases," *Journal of the American Chemical Society*, vol. 85, no. 22, pp. 3533–3539, 1963.

[55] T.-L. Ho, "Hard soft acids bases (HSAB) principle and organic chemistry," *Chemistry Review*, vol. 75, no. 1, pp. 1–20, 1975.

[56] L. Zhang, R. He, and H.-C. Gu, "Oleic acid coating on the monodisperse magnetite nanoparticles," *Applied Surface Science*, vol. 253, no. 5, pp. 2611–2617, 2006.

[57] N. V. Jadhav, A. I. Prasad, A. Kumar et al., "Synthesis of oleic acid functionalized Fe_3O_4 magnetic nanoparticles and studying their interaction with tumor cells for potential hyperthermia applications," *Colloids and Surfaces B: Biointerfaces*, vol. 108, pp. 158–168, 2013.

[58] A. K. Singh, V. Viswanath, and V. C. Janu, "Synthesis, effect of capping agents, structural, optical and photoluminescence properties of ZnO nanoparticles," *Journal of Luminescence*, vol. 129, no. 8, pp. 874–878, 2009.

[59] D. S. Ginger and N. C. Greenham, "Charge injection and transport in films of CdSe nanocrystals," *Journal of Applied Physics*, vol. 87, no. 3, pp. 1361–1368, 2000.

[60] J. Seo, W. J. Kim, S. J. Kim, K. S. Lee, A. N. Cartwright, and P. N. Prasad, "Polymer nanocomposite photovoltaics utilizing CdSe nanocrystals capped with a thermally cleavable solubilizing ligand," *Applied Physics Letters*, vol. 94, no. 13, article 133302, 2009.

[61] J. Huang, B. Xu, C. Yuan et al., "Improved performance of colloidal CdSe quantum dot-sensitized solar cells by hybrid passivation," *ACS Applied Materials & Interfaces*, vol. 6, no. 21, pp. 18808–18815, 2014.